

Cold matter trapping via slowly rotating helical potential.

A.Yu.Okulov*

Russian Academy of Sciences, 119991, Moscow, Russia

(Dated: September 3, 2010)

We consider nonlinear flows of the cold bosonic ensemble trapped by a helical interference pattern in the optical *loop* scheme. Two counter propagating Laguerre-Gaussian laser beams (LG) with a slightly detuned frequencies produce rotating helical potential provided their orbital angular momenta $\pm\hbar\ell$ are counter directed. The small frequency difference $\delta\omega$ required for helix rotation might be induced by rotational Doppler effect. The superfluid hydrodynamics is analysed for the large number of atoms trapped by a slowly rotating helical optical potential in Thomas-Fermi approximation. For the highly elongated trap the Gross-Pitaevskii equation is solved in slowly varying envelope approximation. The speed of axial translation and angular momentum of interacting atomic cloud are evaluated. In the $T \rightarrow 0$ limit the angular momentum of the helical cloud is expected to be zero while toroidal trapping geometry leads to $2\hbar$ angular momentum per trapped atom.

PACS numbers: 37.10.Gh 42.50.Tx 67.85.Hj 42.65.Hw

I. INTRODUCTION

The hydrodynamics of the sufficiently cold ($T \sim 10^{-6}K$) bosonic ensemble trapped by optical potential $V(\vec{r}, t)$ [1–3] follows to Gross-Pitaevskii equation (GPE) [4]:

$$i\hbar \frac{\partial \Psi}{\partial t} = -\frac{\hbar^2}{2m} \Delta \Psi + V(\vec{r}, t) \Psi + \frac{4\pi\hbar^2 a_s}{m} |\Psi|^2 \Psi, \quad (1)$$

where m is the mass of atom. The interaction of atoms leads to the remarkable many-body effects governed by the sign and magnitude of the scattering length : the negative a_s reduces the energy of ensemble and causes the mutual attraction of atoms. This results in formation of bright solitons in **1D** and collapse in higher dimensions. On the contrary at positive a_s atoms repel each other and dark solitons or vortices are formed. In the presence of periodic potential gratings [5]:

$$V(\vec{r}, t) \sim I(z, r, \theta, t) \sim \exp[-r^2] \cos[\delta\omega t - (k_f + k_b)z], \quad (2)$$

where r is a distance from propagation axis z , $\delta\omega = c \cdot (k_f - k_b) = \omega_f - \omega_b$ is a frequency difference of the counter-propagating z -paraxial laser beams with the opposite wave vectors $|\vec{k}_{(f,b)}| \approx k_{(f,b)}$, the many-body nonlinearity leads to the nonlinear tunneling, self-trapping and other quantum interference phenomena [6]. For accelerated **1D** optical gratings when $\delta\omega = \delta\omega \cdot t$, i.e. in the non inertial reference frames [5] the interacting bosons demonstrate Bloch oscillations and Landau-Zener tunneling.

The goal of present work is to study bosonic ensemble in rotating reference frame by virtue of rotating optical *dipole* trap, where rotation is induced by frequency

detuning $\delta\omega$. The proposed trap configuration is composed of the two counter propagating optical vortices. The shape of the interference pattern is defined by mutual orientation of their orbital angular momenta(OAM). When angular momenta are co-directed the $\lambda/2$ spaced *toroidal* traps are formed by LG vortices as already had been used for the single atom trapping and detection [7] and for the persistent condensate flows in toroidal beam waist of LG beam [8]. When orbital angular momenta are counter directed which happens due to the phase-conjugation of the backward reflected LG beam [9] the **1D** sinusoidal intensity grating is transformed into the truly **3D helicoidal** (fig. 1) grating $I(z, r, \theta, t)$ [10] as is shown in Sec.II [11–13]:

$$I(z, r, \theta, t) \cong r^2 \exp[-r^2] \cos[\delta\omega t - (k_f + k_b)z + 2\theta], \quad (3)$$

where z, r, θ are cylindrical coordinates collocated with a propagation axis z . The counter propagating Bessel beam vortices are also capable to confine an atomic ensemble into the helical and toroidal waveguides [14] when their OAM's are properly oriented.

The rotation of helical potential is equivalent to the rotation of the reference frame. We use dipole force [3] rather than Zeeman sublevels which are essential for the previously realized optical interferometric configurations developed for polarization gradient cooling [15], where the laser beams with counter directed *spin* angular momenta (circular polarizations) produce static potential gratings and this is used for the sub-Doppler deceleration of the atomic beam. This analysis is complementary to already performed experiments on condensate dragging in a fast rotation of pancake (**2D**) traps [1] or accelerating 1D traps [5]. The rotating triangular and square optical lattices are capable to pin the vortices of cold boson at the antinodes (under *blue* detuning) of the optical interference pattern, but the perfect collocation was not observed [16].

In the absence of rotation a deep optical lattice maintains the long range order of condensate, but when potential is switched off the vortex-antivortex pairs emerge in

*Electronic address: alexey.okulov@gmail.com;
URL: <http://okulov-official.narod.ru>

accordance with the Berezinskii-Kosterlitz-Thouless scenario [2]. Strictly speaking the optical lattices also contain singularities placed at the nodes of interference pattern [17]. Thus in a certain situation the optical torque may involve atoms in rotation around zeros of optical field: this process is expected to produce stable vortex-antivortex atomic lattices. The other relevant mechanism is the static *hexagonal* lattice formation by interference of the three-way segmented nonrotating condensate [18].

In sec.III we analyze the light orbital angular momentum in the purely *linear* optical setup (fig. 2) [13] where the phase conjugation of LG beams is performed. The helical interference patterns (3) is formed therein without conventional nonlinear optical phase conjugators [12]. The frequency splitting of the order of $\delta\nu \cong 10^{-1-2} \text{ Hz}$ of the counter propagating LG may occur due to rotational Doppler effect [19, 20] which is the cause of the slow rotation of the helical interference pattern around LG propagation axis [9].

In the sec.IV we consider two possible regimes of the cold atomic ensemble trapping when kinetic energy of atomic ensemble is small compared to the interaction and trapping energies. One solution is obtained as a balance of the red-detuned optical potential attraction and self-defocusing due to positive a_s . It has atomic density ρ_{helix} perfectly collocated with rotating optical helix $I(z, r, \theta, t)$. In this case the rotating potential imposes rotation to superfluid. The other TFA solution has non-rotating density "funnel" profile ρ_{fun} .

The sec.V presents the analytical solution of GPE for nonzero kinetic energy, provided that optical trapping energy and interaction energies cancel each other. In sec.VI the linear momentum $\langle P_z \rangle$ and angular momentum $\langle L_z \rangle$ of this helical ensemble are evaluated. The Landau criterion $|\vec{V}| > \epsilon(\vec{p})/|\vec{p}|$ for the appearance of elementary excitations and superfluidity breakup [21] is discussed for helical geometry (fig. 1,fig. 3).

II. HELICAL INTERFERENCE PATTERN

It is well known that interference of a two counter propagating plane waves with a slightly different frequencies ω_f, ω_b produces a running sinusoidal *roll* intensity grating [6, 26]. For the equal wave amplitudes $|\mathbf{E}_f|, |\mathbf{E}_b|$ and the phase difference ϕ the distribution of the light intensity $I(z, r, \theta, t)$ has the following form:

$$I(z, r, \theta, t) \sim 2|\mathbf{E}_{(f,b)}|^2 [1 + \cos[\delta\omega t - (k_f + k_b)z + \phi]] \exp[-\frac{r^2}{D_0^2(1+z^2/z_R^2)}], \quad z_R = k_{(f,b)}D_0^2, \quad (4)$$

provided that a visibility of pattern is good enough $|\mathbf{E}_{(f)}| \cong |\mathbf{E}_{(b)}|$ [24], where z_R is Rayleigh range, D_0 is a beam waist radius, the self-similar variable $\chi = (\omega_f - \omega_b)t - (k_f + k_b)z + \phi$ is responsible for the translation of the interference pattern along z axis with the group velocity $V_z = (\omega_f - \omega_b)/(k_f + k_b)$. The transversal

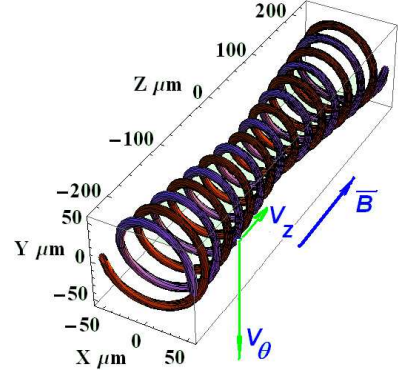


FIG. 1: The isosurface of the optical intensity I_{tw} and the Thomas-Fermi density ρ_{tw} of the cold atomic cloud in a helical optical dipole trap (7,18) (the scales are in μm , but longitudinal modulation of $\lambda/2$ is enlarged). The spatial modulation is induced by the interference of counter-propagating LG beams with the opposite angular momenta. The pattern rotates with angular frequency $\delta\omega$ as a "solid-body". Magnetic field \vec{B} adjusts the scattering length a_s to balance the attractive optical potential by many body defocusing.

(in the plane (r, θ)) confinement of the light amplitudes $\mathbf{E}_f, \mathbf{E}_b$ is typical for the zeroth-order Gaussian beams. The *roll* interference pattern evolves into the sequence of the equidistantly spaced rotationally invariant (in θ) *ellipsoids* centered at the propagation axis z [9]. For the higher-order propagation modes namely Laguerre-Gaussian beams (LG) with azimuthal quantum number ℓ and orbital angular momentum $\ell\hbar$ per photon [25]:

$$\mathbf{E}_{(f,b)}(z, r, \theta, t) \sim \frac{\mathbf{E}_{(f,b)} \exp [i(-\omega_{(f,b)}t \pm k_{(f,b)}z) \pm i\ell\theta]}{(1+iz/z_R)} (r/D_0)^{|\ell|} \exp [-\frac{r^2}{D_0^2(1+iz/z_R)}], \quad (5)$$

the interference pattern is different for LG reflected from conventional mirror and phase conjugating mirror. Backward reflection from conventional spherical mirror changes the topological charge of the LG [9], exactly in the same way as circular polarization of light changes from left to right and vice-versa in reflection [26]. The intensity $I_{tor}(z, r, \theta, t)$ vanishes on the beam axis thus interference pattern transforms into the sequence of the equidistant rotationally invariant *toroids* separated by $\lambda/2$ interval:

$$I_{tor}(z, r, \theta, t) = A_n \cdot [1 + \cos[\delta\omega \cdot t - (k_f + k_b)z]] (r/D_0)^{2|\ell|} \exp[-\frac{2r^2}{D_0^2(1+z^2/z_R^2)}], \quad A_n = \epsilon_0 c \frac{2|\mathbf{E}_{(f,b)}|^2 2^{(|\ell|+1)}}{\pi \ell! D_0^2}, \quad (6)$$

where ϵ_0 is the dielectric permittivity of vacuum. The reflection from phase-conjugating mirror (PCM) does not change the topological charge of LG and the interference

pattern is twisted [9, 12]:

$$I_{tw}(z, r, \theta, t) = [1 + \cos[\delta\omega \cdot t - (k_f + k_b)z + 2\ell\theta]] \times A_n \cdot (r/D_0)^{2|\ell|} \exp\left[-\frac{2r^2}{D_0^2(1+z^2/z_R^2)}\right]. \quad (7)$$

The intensity also vanishes at LG axis z as $r^{2|\ell|}$, while a self-similar argument:

$$\chi = [(\omega_f - \omega_b)t - (k_f + k_b)z + 2\ell\theta], \quad (8)$$

keeps the maxima of intensity at the 2ℓ collocated helices separated from each other by $\lambda/2$ interval (fig. 1). The azimuthal term $2\ell\theta$ appears due to phase conjugation $\mathbf{E}_b \sim \mathbf{E}_f^*$. Thus we have the following strict correspondence between the *roll* interference pattern (2) and the helical interference pattern (7): the frequency difference $\delta\omega = \omega_f - \omega_b$ is the cause of the translation of *rolls* with *group* velocity $V_z = (\omega_f - \omega_b)/(k_f + k_b)$ of the wavetrain, produced by a sum of the two counter-propagating beams ($\mathbf{E}_f + \mathbf{E}_b$) [5]. The $\delta\omega$ is responsible also for the rotation of *helices* with angular velocity $\dot{\theta} = \delta\omega/2\ell$. The rotation is the cause of the *pitch* of helical interference maxima along z -axis. Consequently there exists a perfect mechanical analogy between the *solid body* rotation of the helix described by formula (7) and an Archimedean screw. Namely the positive $\delta\omega$ corresponds to the counter-clockwise rotation and this provides the *pitch* in positive z direction for *right* helices. On the other hand the negative $\delta\omega$ means clockwise rotation. In this case ($\delta\omega < 0$) the positive translation speed in z direction takes place for the *left*-handed helices. Evidently the change of the topological charge ℓ changes the direction of helix translation \vec{V}_z due to alternation of the helix hand to the opposite one for a given $\delta\omega$.

This mechanical analogy is useful for the analysis of the cold atoms motion in the helical trap. The velocity vector of the condensate fragment trapped and perfectly collocated with intensity maxima has two components $\vec{V} = \vec{V}_z + \vec{V}_\theta$ (fig. 1). The axial component is a *group* velocity $|\vec{V}_z| = (\omega_f - \omega_b)/(k_f + k_b)$ of the wavetrain, while the azimuthal component $|\vec{V}_\theta| = (\omega_f - \omega_b) \cdot D_0$ is of kinematic nature. Such a *solid body* field of velocities is reminiscent to the rotation of a *classical* liquid together with rotating container [27, 28] where the angular velocity $\delta\omega(r)$ is the r -independent constant. Noteworthy the *effective* field of velocities $\vec{V} = \hbar\nabla\theta/m$ of the optical LG vortex (5) is of different nature and this effective velocity field is equivalent to those of quantum liquid composed of particles of mass m which have orbital angular momentum $L_z = mV_\theta r = \ell\hbar$ independent of r [27]. As is well known the velocity $V_\theta(r) \sim r^{-1}$ and the angular velocity $\omega(r) \sim r^{-2}$ fields of the vortex inside quantum liquid have the point singularities at the vortex core ($r \rightarrow 0$).

III. LINEAR OPTICAL LOOP PHASE-CONJUGATION

The apparent topological difference of toroidal (6) and helicoidal (7) interference patterns is due to the mutual orientation of their orbital angular momenta. The toroidal pattern appears when colliding photons have a parallel OAM's [7] while helicoidal pattern [9] arises for antiparallel OAM's. This follows from direct calculation of OAM for the ℓ 'th order LG. The OAM is the expectation value of the angular momentum operator $\hat{L}_z = -i\hbar[\vec{r} \times \nabla] = -i\hbar\frac{\partial}{\partial\theta}$ inside the interaction volume $V \cong \pi D_0^2 z_R$ [29, 30]:

$$\begin{aligned} < L_z >_{(f,b)} &= < \Psi_{(f,b)}^\ell | \hat{L}_z | \Psi_{(f,b)}^\ell > \\ &= 2\epsilon_0 \int_V (E_{(f,b)}^+)^* (-i\hbar[\vec{r} \times \nabla] E_{(f,b)}^+) d^3\vec{r} = \\ &\int (E_{(f,b)}^+)^* (-i\hbar\frac{\partial}{\partial\theta} E_{(f,b)}^+) r dr \cdot d\theta dz \simeq \pm\ell\hbar\frac{I_{(f,b)}V}{\hbar\omega_{(f,b)}c}, \end{aligned} \quad (9)$$

where $I_{(f,b)} = \epsilon_0 c |\mathbf{E}_{(f,b)}|^2$ is the light intensity, $\Psi_{(f,b)}^\ell = \sqrt{2\epsilon_0} E_{(f,b)}^+(z, r, \theta, t)$ are the macroscopic wavefunctions of a single light photon inside a forward (*f*) or backward (*b*) LG wavetrains (5) with the winding number ℓ . The interaction volume V is located near $z = 0$ plane within Rayleigh range $z < z_R$ and the fields $E_{(f,b)}^+$ are both calculated inside this volume (fig.2). The square modulus $|\Psi_{(f,b)}^\ell|^2$ is a probability density of photon detection which is proportional to the energy density of classical wave. This is a Sipe's single-photon wavefunction [30] which is proportional to the positive frequency part $E_{f,b}^+$ of the counter-propagating classical optical fields. The usage of the nonrelativistic operators of the linear momentum (\hat{P}) and angular momentum \hat{L}_z is justified by the applicability of the paraxial approximation to the slowly diverging LG beams. In this particular paraxial case the spin-orbit coupling [29] may be neglected and the angular momentum of the photon is exactly decoupled to the spin and the orbital component: $\hat{J} = \hat{S} + \hat{L}$. The linear momentum expectation values for the forward and backward LG's respectively are obtained in following way:

$$\begin{aligned} < P_z >_{(f,b)} &= < \Psi_{(f,b)}^\ell | \hat{P} | \Psi_{(f,b)}^\ell > = 2\epsilon_0 \times \\ &\int (E_{(f,b)}^+)^* (-i\hbar\frac{\partial}{\partial z} E_{(f,b)}^+) d^3\vec{r} \simeq \pm\hbar k_{(f,b)} \frac{I_{(f,b)}V}{\hbar\omega_{(f,b)}c}. \end{aligned} \quad (10)$$

The ratio of the angular and linear momenta is $L_z/P_z \sim \ell c/\omega_{(f,b)}$ [31]. The simplest conceivable configuration of linear PCM composed of plane mirrors, wavefront curvature compensating lenses and beam splitters is shown at fig.2. The goal of proposed setup is to counter-direct the splitted LG beams. The four reflections are the necessary minimum. The case is that the incidence angles much above 45 degrees will distort both polarization and spatial structure of LG. In addition a small sliding of a

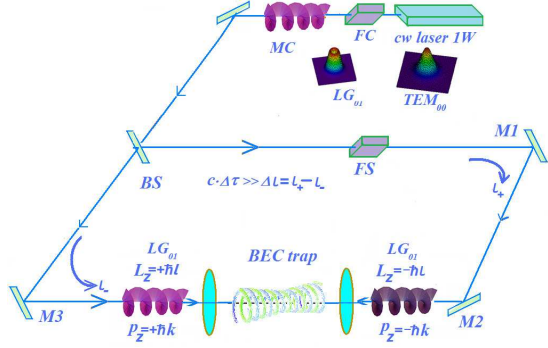


FIG. 2: The closed loop setup for producing the helical interference pattern. The CW laser emits fundamental mode which passes through Faraday isolator (FC). The mode-converter MC made of the two cylindrical lenses [31] transforms the fundamental Gaussian mode into LG beam with topological charge ℓ . Frequency shifter FS might be acoustooptic cell, rotating $\lambda/2$ plate or Dove prism. The parabolic wavefront curvatures due to the free-space diffraction are compensated by thin lenses.

beam along the reflecting surface [32] may occur when mirror is tilted with respect to the LG propagation axis. The evident physical restriction on this *loop* setup is to keep the path difference ΔL of the counter directed LG smaller than coherence length of trapping laser field ($\Delta L << c\tau_{coh}$) (fig.2) [13]. The small frequency shift $\delta\omega \approx 2\pi \cdot 10^{-(1-3)} \text{rad/sec}$ required to cause the helix rotation [9] might be induced by a frequency ramp [5] or via rotational Doppler shift which appears due to rotation of the half-wavelength plate [19] or Dove prism [20].

IV. MACROSCOPIC WAVEFUNCTIONS FOR A COLD BOSONS IN A RED-DETUNED HELICAL TRAPS.

Consider a bosonic cloud prepared in an elongated trap [5] and suddenly released afterwards. The well elaborated experimental procedure is to impose a periodic optical potential to study the Bloch oscillations, macroscopic Landau-Zener tunneling and Josephson effects [6, 22]. In our case the imposed optical potential is *helical*:

$$V_{opt}(z, r, \theta, t) = -\frac{\text{Re}[\alpha(\omega)]}{2\epsilon_0 c} I_{tw}(z, r, \theta, t),$$

$$\alpha(\omega) = 6\pi\epsilon_0 c^3 \frac{\Gamma/\omega_0^2}{(\omega_0^2 - \omega^2 - i(\omega^3/\omega_0^2)\Gamma)}, \quad (11)$$

where $\alpha(\omega)$ is the polarizability of atom, which is real, i.e. $\alpha(\omega) \approx \text{Re}[\alpha]$ at large detunings from resonance $\omega - \omega_0$, $\Gamma = e^2\omega_0^2/6\pi\epsilon_0 m_e c^3$ is classical damping rate via radiative energy loss, m_e is electron mass [3, 17]. The GPE for the macroscopic BEC wavefunction Ψ confined

by V_{opt} is:

$$i\hbar \frac{\partial \Psi(\vec{r}, t)}{\partial t} = -\frac{\hbar^2}{2m} \Delta \Psi + V_{opt} \Psi + \frac{4\pi\hbar^2 a_s(\vec{B})}{m} |\Psi|^2 \Psi, \quad (12)$$

with $a_s(\vec{B}) = a_{bg}(1 + \Delta_B/(\lvert \vec{B} \rvert - B_F))$ magnetic field dependent s -wave scattering length, where a_{bg} is background value of a_s , B_F and Δ_B are the Feshbach magnetic induction and resonance width respectively.

The helical trapping configuration offers a certain difficulties in searching both the ground state Ψ_0 and an excited states. For the sake of preliminary analysis let us look for the ultimately simplified solutions. Namely for the sufficiently large number of trapped atoms ($N \cong 10^{9-12}$) the quantum pressure term which follows from the uncertainty principle is small ($\hbar^2 \Delta \Psi / 2m \sim 0$) compared to the optical trapping and interaction terms (second and third terms in the right side of eq.(12)). Thus standard condition for the neglection of kinetic energy is [4]:

$$\frac{E_{int}}{E_{kin}} \cong \frac{N \cdot a_{bg}}{a_{ho}}, \quad (13)$$

where $a_{ho} \cong \sqrt{\hbar/m\omega_z} \sim \lambda/2$ is the "harmonic oscillator width" [4] and the atomic density $\rho = N/V_H$ is averaged over the above defined helical trap volume $V_H = \pi D_0^2 z_R$. According to (13) the ratio E_{int}/E_{kin} must be much more than unity for the most of the near infrared lasers $\lambda = 0.8 - 1.5 \mu\text{m}$, under the standard focusing requirement $D_0 \sim 10 - 100 \mu\text{m}$ and under the experimentally achievable tuning of $a_s(\vec{B})$ in the range $\cong 1 - 100 \text{nm}$ via Feshbach resonance. For the mid-infrared trapping at carbon dioxide lasing wavelength $\lambda = 10.6 \mu\text{m}$ the kinetic energy term $E_{kin} = 2\hbar^2/m\lambda^2$ is about 100 times smaller. The optical dipole trapping energy E_{dipole} is:

$$E_{dipole} \cong N \cdot V_{opt} \cong -\frac{\vec{p} \cdot \vec{E}}{2} \cong \frac{-\alpha \vec{E}^2 N}{2}$$

$$\cong \frac{-\alpha I_{tw} N}{2\epsilon_0 c} = \frac{-e^2 I_{tw} N}{m_e \Delta \omega^2 2\epsilon_0 c}, \quad \Delta \omega = \omega_{f,b} - \omega_0 \quad (14)$$

where I_{tw} is the optical intensity of trapping beams. We have used here the universal form of electric dipole transition applicable to alkali atoms with a few percent accuracy [3]. Hence one might expect that a Thomas-Fermi approximation (TFA) is valid in our case when interaction is repulsive, i.e. for the positive a_s [4]. The magnitude and sign of the scattering length a_s are flexible parameters due to the externally applied magnetic induction \vec{B} for the alkali atoms alike *Li*, *Na*, *K*, *Rb*, *Cs* [22].

The following estimates will be done for simplicity in the vicinity of the LG-beam waist, i.e. within Rayleigh range, when $z < z_R$. Consider first the following TFA wavefunction which satisfies the GPE (12):

$$\Psi_{fun} = \Phi(r) \exp \left[-\frac{i\mu(r)t}{\hbar} + i\Phi(r)^2 \sin(\delta\omega t - 2k_z z + 2\ell\theta) \right], \quad (15)$$

where $\mu(r)$, a local r -dependent chemical potential is:

$$\mu(r) = 4\pi\hbar^2 a_s \Phi(r)^2/m; \quad I_{tw} = 2\epsilon_0 c |\mathbf{E}_{(f,b)}|^2; \\ \Phi(r)^2 = \exp(-2r^2/D_0^2) \cdot (r/D_0)^{2|\ell|} \cdot \frac{\alpha(\omega) I_{tw}}{2\epsilon_0 c \cdot \hbar \cdot \delta\omega}. \quad (16)$$

The wavefunction (15) is normalizable and fits the GPE by direct substitution. In particular the TFA density of atoms $\rho_{fun}(z, r, \theta, t) = |\Psi_{fun}|^2 = \sim \exp(-2(r/D_0)^2)/(r/D_0)^{2|\ell|}$ is (z, t) -independent "funnel" collocated with the optical helix $I_{tw}(z, r, \theta, t)$. The phase modulation of Ψ_{fun} has a maximum near the density maximum $\rho_{fun}(z, r, \theta, t)$, sinusoidal dependence on azimuthal angle θ and decreases down to zero on LG axis and outside the LG waist. Noteworthy Ψ_{fun} is a multiply valued function of θ . Hence this solution might be of highly restricted interest only, e.g. for evaluations of the thermodynamical parameters of the cold ensemble with $|\Psi_{fun}|^2$ density profile as the other TF solutions are typically used [4].

The other solution in TF approximation is obtained for r -independent chemical potential $\mu = const$. For this solution the mean field wavefunction Ψ_h is a sum of the two phase-conjugated wavefunctions with the opposite angular momenta $\pm\hbar\ell$:

$$\Psi_h(z, r, \theta, t) = \Psi_\ell(z, r, \theta, t) + \Psi_{-\ell}(z, r, \theta, t) \cong \\ \Psi_{\pm\ell}(z=0) \cdot \frac{(r/D_0)^{|\ell|}}{1+z^2/z_R^2} \exp \left[-\frac{r^2}{D_0^2(1+iz/z_R)} \right] \times \\ \left\{ \frac{\exp[-i\mu_f t/\hbar + ik_f z + i\ell\theta]}{(1+iz/z_R)} + \frac{\exp[-i\mu_b t/\hbar - ik_b z - i\ell\theta]}{(1+iz/z_R)} \right\}, \quad (17)$$

where the difference of the partial chemical potentials $(\mu_f - \mu_b)$, associated with the each of "counter-propagating" wavefunctions $\Psi_\ell, \Psi_{-\ell}$ is adjusted to the frequency difference of counter-propagating optical fields $(\mu_f - \mu_b)/\hbar = \delta\omega = \omega_f - \omega_b$. The substitution of this TFA wavefunction into GPE gives the following link for parameters:

$$\mu - \frac{\alpha(\omega) I_{tw}(0) \cdot [1 + \cos(\delta\omega t + 2kz \pm 2\ell\theta)]}{2\epsilon_0 c \cdot g (1+z^2/z_R^2)} (r/D_0)^{2|\ell|} \times \\ \exp \left[-\frac{2r^2}{D_0^2(1+z^2/z_R^2)} \right] = \rho_{helix}(z, r, \theta, t), \quad (18)$$

where $k = k_f \cong k_b$, $\mu = \mu_f \approx \mu_b$ is a constant (z, r, θ, t -independent) value of chemical potential, $g = 4\pi\hbar^2 a_s(\vec{B})/m$ is the interaction parameter. This equation means the quasiclassical restriction imposed on a homogeneity of chemical potential of the system in an external field V_{opt} [4]. In accordance to this solution the density of the cold atomic ensemble $\rho_{helix}(z, r, \theta, t)$ is perfectly correlated with the rotating optical helix potential $I_{tw}(z, r, \theta, t)$ as depicted at fig.1. The density ρ_{helix} rotates as a "solid body" with a pitch of the $\lambda/2$. The speed of the axial translation is $V_z = \lambda \cdot \delta\omega/4\pi$.

V. EXACT HELICAL SOLUTION FOR NONZERO KINETIC ENERGY

Apart from TF approximation the truly exact solution with nonzero kinetic energy exists $\Psi_{ex} = \Psi_f + \Psi_b$ which is also a superposition of the two counter propagating *paraxial* matter waves Ψ_f and Ψ_b . Let us reduce GPE (12) to the "paraxial form" relevant to highly elongated geometry, as a *helical* one in our case:

$$i\hbar \frac{\partial \Psi_{(f,b)}}{\partial t} = -\frac{\hbar^2}{2m} \Delta_\perp \Psi_{(f,b)} - i \frac{2k_{(f,b)}\hbar^2}{2m} \frac{\partial \Psi_{(f,b)}}{\partial z} + V_{opt} \Psi_{(f,b)} \\ + \frac{\hbar^2}{2m} k_{(f,b)}^2 \Psi_{(f,b)} + \frac{4\pi\hbar^2 a_s(\vec{B})}{m} |\Psi_f + \Psi_b|^2 \Psi_{(f,b)}, \quad (19)$$

The perfect mutual cancellation of trapping and interaction terms:

$$-V_{opt}(z, r, \theta, t) \Psi_{(f,b)} = \frac{4\pi\hbar^2 a_s(\vec{B})}{m} |\Psi_f + \Psi_b|^2 \Psi_{(f,b)}, \quad (20)$$

occurs when nonlinear defocusing due to positive scattering length a_s is compensated by attraction to intensity maxima caused by red detuning.

Taking again the exact helical solution of (19) as a superposition of the two counter-propagating vortices:

$$\Psi_{ex}(z, r, \theta, t) = \Psi_f(z, r, \theta, t) + \Psi_b(z, r, \theta, t) \cong \\ \tilde{\Psi}_f \cdot \exp[-\frac{i\mu_f t}{\hbar} + ik_f z] + \tilde{\Psi}_b \cdot \exp[-\frac{i\mu_b t}{\hbar} - ik_b z], \quad (21)$$

and under the natural assumptions:

$$(17) \quad k_{(f,b)} \frac{\partial \tilde{\Psi}_{(f,b)}}{\partial z} \gg \frac{\partial^2 \tilde{\Psi}_{(f,b)}}{\partial z^2}, \quad (22)$$

two following equations for counter propagating and counter rotating matter waves $\tilde{\Psi}_f$ and $\tilde{\Psi}_b$ are valid:

$$i 2k_{(f,b)} \frac{\partial \tilde{\Psi}_{(f,b)}}{\partial z} + \Delta_\perp \tilde{\Psi}_{(f,b)} - (k_{(f,b)}^2 + 2m\mu_{(f,b)}/\hbar^2) \Psi_{(f,b)} = 0, \quad (23)$$

which have the vortex solutions with charge ℓ for the $\tilde{\Psi}_{f,b}(z, r, \theta)$ with initial condition at $z = 0$ equals $\tilde{\Psi}_0$:

$$\tilde{\Psi}_{(f,b)} \sim \frac{\tilde{\Psi}_0 \cdot (r/D_0)^{|\ell|} \cdot \exp \left[-\frac{r^2}{D_0^2(1+iz/z_R)} \pm i\ell\theta \right]}{(1+iz/z_R)}. \quad (24)$$

The issues of dynamical stability of (21) with respect to small [16] perturbations and thermodynamical stability from the point of view of least energy arguments deserve a further careful analysis and will be published elsewhere.

VI. DISCUSSION

The helical solutions composed of the counter propagating free space LG wavefunctions apparently fit to the continuity equation and have realistic field of velocities.

The one possible application of the (15,17, 21) might be in using them as variational anzatz for emulation of GPE [33]. Nevertheless the explicit form of solutions (17,21) offers a possibility to evaluate the significant macroscopic observables of the trapped ensemble. The situation is the same as in the case of the wavetrain composed of the two counter propagating LG vortices, considered in Sec.II and Sec.III. The *helical* TFA solution Ψ_h (17) has nonzero momentum P_z :

$$\begin{aligned} \langle P_z \rangle_h &= \langle \Psi_h | -i\hbar \frac{\partial}{\partial z} | \Psi_h \rangle = N\hbar(k_f - k_b) \Leftarrow \hbar \int_V dV \cdot \\ &\exp(-r^2)r^{2|\ell|}[k_f - k_b + k_f \exp(i\chi) - k_b \exp(-i\chi)], \end{aligned} \quad (25)$$

and easily calculated angular momentum L_z :

$$\begin{aligned} \langle L_z \rangle_h &= \langle \Psi_h | -i\hbar \frac{\partial}{\partial \theta} | \Psi_h \rangle = N\ell\hbar(1 \mp 1) \Leftarrow \\ \hbar \int_V dV \exp(-r^2)r^{2|\ell|} &[1 \mp 1 + \exp(i\chi) \mp \exp(-i\chi)], \end{aligned} \quad (26)$$

in accordance with standard procedure performed in Sec.III for the linear (10) and angular momenta (9) of optical vortices and due to apparent identity $\int_0^{2\pi} \sin(\chi)d\theta = 0$. Here in (26) the upper \mp sign corresponds to counter directed angular momenta and helical interference pattern (7), while bottom \mp sign corresponds to the toroidal optical interference pattern (6).

The same expectation values $\langle P_z \rangle_{ex} = N\hbar(k_f - k_b)$ and $\langle L_z \rangle_{ex} = N\ell\hbar(1 \mp 1)$ has exact wavefunction $\Psi_{ex}(21)$. Quantum mechanically this happens because the wavefunction in both cases is a superposition of the two partial matter waves Ψ_f and Ψ_b (21) (or Ψ_ℓ and $\Psi_{-\ell}(17)$) having opposite and quantized (i.e. equal to $\pm\ell\hbar$) mutually subtracted angular momenta. This means also that helical wavetrain (7) contains OAM of exactly $0 \times \ell\hbar$ per photon, while toroidal wavetrain (6) contains $2\ell\hbar$ per photon.

This feature looks seemingly counter intuitively from the point of view of classical hydrodynamics. Namely the density of atomic ensemble $\rho_{helix} = |\Psi_{h,ex}|^2$ rotates as a *solid body* and one might expect that ρ_{helix} to have classically the angular momentum $L_{class} = I_{zz} \cdot \delta\omega$, where I_{zz} is the moment of inertia of the helical *wire* located in LG beam waist with the density profile ρ_{helix} [34]:

$$\begin{aligned} I_{zz} &= \int Nm|\Psi_{h,ex}|^2 r^2 dV = Nm \int |\Psi_{h,ex}|^2 r^3 dr d\theta dz \simeq \\ &\sim Nm \int (1 + \cos(\delta\omega t + (k_f + k_b)z + 2\ell\theta)) \cdot d\theta dz \cdot \\ &\exp(-r^2/D_0^2)r^{2+2|\ell|} \cdot rdr \sim NmD_0^2 Z_r. \end{aligned} \quad (27)$$

Nevertheless due to the basic property of angular momentum, namely the *quantization* of the angular momentum in free space, the oppositely directed angular momenta cancel each other completely, because they have integer opposite values of $\pm\ell\hbar$ [35]. On the contrary, the linear momentum is *not* quantized in free space

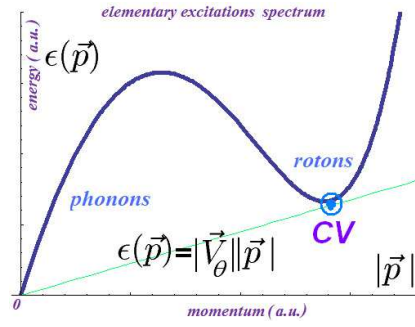


FIG. 3: Landau criterion for superfluidity for helical trap. Roton minimum touches the straight line $|\vec{V}_\theta||\vec{p}|$ which corresponds to superfluid regime destruction by means of roton excitation when critical velocity (CV) reached.

and this leads to nonzero net linear momentum P_z of the ensembles (17,21), regardless to the mutual orientation of their OAM's. The net momentum P_z is small because of the smallness of the *group* velocity of the helical wavetrain $V_z = \delta\omega/(k_f + k_b)$. For example when frequency splitting $\delta\omega$ is induced by rotational Doppler effect [13, 19], the speed of the axial translation of the helical density profiles (17,21) is $V_z \sim$ several μm per second (several rotations of helix per second). The azimuthal velocity $V_\theta = \delta\omega \cdot D_0$ is about two orders of magnitude bigger due to $D_0/\lambda \sim 10^2$, but rotational contribution to kinetic energy E_{kin} is zero. The net angular momentum of the helical wavetrains (17, 21) is zero in $T \rightarrow 0$ limit [4] because only superfluid component remains.

The else interesting physical consequences relevant to experiments with quantum gas in optical traps may be formulated from the point of view of the Landau criterion $|\vec{V}| > \epsilon(\vec{p})/|\vec{p}|$ for the appearance of elementary excitations (rotons) and superfluidity destruction ($\epsilon(\vec{p})$ is the energy - momentum dispersion relation). Following to [21, 27] consider the flow of quantum gas in a narrow channel with velocity $\vec{V} = \vec{V}_z + \vec{V}_\theta$. In the rest frame the momentum of excitation \vec{p} ought to be opposite to the velocity of superfluid \vec{V} , because of the least energy constraint imposed upon excitation $\epsilon(\vec{p}) + \vec{p} \cdot \vec{V} < 0$. Thus $\epsilon(\vec{p}) - |\vec{p}| \cdot |\vec{V}| < 0$ and $|\vec{V}| > \epsilon(\vec{p})/|\vec{p}|$. Because in our case the only significant component of \vec{V} is $V_\theta = \delta\omega D_0$, the condition of appearance of excitation with momentum \vec{p} reads as:

$$\delta\omega_{crit} D_0 > \epsilon(\vec{p})/|\vec{p}|. \quad (28)$$

The experimentally controllable detuning $\delta\omega$ of counter propagating waves ω_f and ω_b by rotational Doppler effect which leads to the change the angular velocity of helix rotation makes possible to determine the critical velocity of superfluid, defined by contact point of roton minimum of $\epsilon(\vec{p})$ (fig. 3) with the line $|\vec{p}|V_\theta$. The turbulent excitations (rotons) are assumed to appear due to ejection of superfluid across the trapping potential barrier owing to centrifugal force, rather than because of the roughness or

the channel end [21, 27].

VII. CONCLUSION AND OUTLOOK

The strongly nonlinear behavior of the trapped degenerate quantum gas in the framework of the Gross-Pitaevskii equation had been studied analytically. The necessary conditions were formulated for the appearance of the helical Bose-Einstein condensate flows due to the Thomas-Fermi balance of the self-defocusing of condensate with positive scattering length a_s and "red" detuned optical dipole force. The minimal achievable ensemble temperature might be approximately evaluated as recoil energy $k_B \cdot T_{recoil} = 4 \cdot \hbar^2 / (2m\lambda^2)$ [15]. The possible experimental implementation of helical trapping is a sudden *switching on* of the helical potential after condensate release from elongated optical trap in a way similar to switching of accelerated grating in Ref. [5].

The peculiarities of the cooling mechanisms in this helical configuration were not considered in the current work. But we hope that a helical (see fig.1) trapping geometry might reveal the new features of the well elaborated mechanisms as a the Doppler cooling [36], polarization gradient cooling [15] or velocity selective population trapping [37]. The newly found loop and helical features of the optical speckle patterns [38, 39] are also a promising trapping opportunities which may enlighten the Anderson localization of cold atoms in 1D and 3D speckle patterns [40].

Noteworthy the similar helical geometry of the colliding LG optical vortices of picosecond duration with opposite angular momenta proposed recently for the plasma currents excitation via ponderomotive force [28]. As the plasma vortices are the sources of the axial magnetic fields, the superfluid motion in helical trapping environment (12) is to be associated with a so-called *artificial* magnetic fields [41, 42].

[1] S.Tung, V.Schweikhard, and E.A.Cornell, Phys.Rev.Lett., **97**,240402 (2006).
[2] S.Tung, V.Schweikhard, and E.A.Cornell, Phys.Rev.Lett., **99**, 030401 (2007).
[3] R.Grimm, M.Weidemuller and Yu.B.Ovchinnikov, Adv.At.Mol.Opt.Phys., **42**, 95 (2000).
[4] F. Dalfovo, S.Giorgini, S.Stringari, L.P.Pitaevskii, Rev.Mod.Phys.,**71**,463(1999).
[5] M. Cristiani, O. Morsch, J. H. Muller, D. Ciampini, and E. Arimondo, Phys.Rev.A, **65**, 063612 (2002).
[6] O.Morsch, M.Oberthaler, Rev.Mod.Phys. **78**, 179 (2006).
[7] T. Puppe, I. Schuster, A. Grotthe, A. Kubanek, K. Murr, P.W.H. Pinkse, and G. Rempe, Phys.Rev.Lett., **99**,013002(2007).
[8] E.R.I.Abraham, J.Tempere and J.T.Devreese, Phys.Rev.A, **64**,023603 (2002).
[9] A.Yu.Okulov, J.Phys.B., **41**,101001 (2008).
[10] M.Bhattacharya, Opt.Commun. **279**, 219 (2007).
[11] A.Yu.Okulov, JETP Lett., **88**, 631 (2008).
[12] M.Woerdemann, C.Alpmann and C.Denz, Opt. Express, **17**, 22791(2009).
[13] A.Yu.Okulov, J. Opt. Soc. Am. B **27**, 2424-2427 (2010).
[14] K.Volke-Sepulveda and R.Jauregui, J.Phys.B., **42**, 085303 (2009).
[15] J. Dalibard and C. Cohen-Tannoudji, J. Opt. Soc. Am. B **6**, 2023(1989).
[16] A.L.Fetter, Rev.Mod.Phys. **81**, 647 (2009).
[17] A.Yu.Okulov, J.Mod.Opt., **55** , 241 (2008).
[18] G.Ruben, D.M.Paganin, M.J.Morgan, Phys.Rev.A, **99**,013002 (2008) .
[19] J. Arlt, M. MacDonald, L. Paterson, W. Sibbett,K. Volke-Sepulveda and K. Dholakia, Opt. Express, **10**(19),844(2002).
[20] Courtial J., Robertson D. A., Dholakia K., Allen L. and Padgett M. J., Phys.Rev.Lett., **81**,4828 (1998).
[21] I.M. Khalatnikov, "An Introduction to the Theory of Superfluidity", Perseus Publishing, Cambridge, MA (2000).
[22] S.Giorgini, L.P.Pitaevskii, S.Stringari, Rev.Mod.Phys. **80**, 1215 (2008).
[23] I.Bloch, J.Dalibard, W.Zwerger, Rev.Mod.Phys. **80**, 885 (2008).
[24] N.G.Basov, I.G.Zubarev, A.B.Mironov, S.I.Mikhailov and A.Y.Okulov, JETP, **52**,847(1980) .
[25] J.Leach,M.J.Padgett,S.M.Barnett,S.Franke-Arnold, and J.Courtial, Phys.Rev.Lett., **88**, 257901(2002).
[26] B.Y.Zeldovich, N.F.Pilipetsky and V.V.Shkunov "Principles of Phase Conjugation",Ch.2, (Berlin:Springer-Verlag)(1985).
[27] R.P.Feynman,"Statistical mechanics", Ch.11,(1972) Reading, Massachusetts,.
[28] A.Yu.Okulov, Phys.Lett.A, **374**,4523-4527 (2010) .
[29] S.M.Barnett, J.Mod.Opt., **57** , 1339-1343(2010) .
[30] J.E.Sipe, Phys.Rev.A, **52**, 1875(1995).
[31] L.Allen, M.W.Beijersbergen, R.J.C.Spreeuw and J.P.Woerdman, Phys.Rev.A, **45**, (1992) 8185-8189.
[32] K.Yu.Bliokh and Yu.P.Bliokh, Phys.Rev.Lett., **96**, 073903(2006) .
[33] B.A.Malomed "Variational methods in nonlinear fiber optics and related fields", Progress in Optics,(E.Wolf, Editor: North Holland, Amsterdam) **43**, 69-191 (2002).
[34] L.D. Landau and E.M. Lifshitz,"Mechanics", Butterworth-Heinemann, Oxford(1976).
[35] M. F. Andersen, C. Ryu, P. Clade, V. Natarajan, A. Vaziri, K. Helmerson, W. D. Phillips, Phys. Rev. Lett., **97**, 170406(2006).
[36] V.S.Letokhov, JETP Lett., **7**, 272(1968). T. W. Hansch and A. L. Schawlow, Opt. Commun. **13**, 68 (1975).
[37] A. Aspect, E. Arimondo, R. Kaiser, N. Vansteenkiste, and C. Cohen-Tannoudji, Phys.Rev.Lett., **61**, 826-829 (1988).
[38] M.R.Dennis, R.P.King, B.Jack, K.O'Holleran, and M.J.Padgett, Nature.Phys.,**6**, 118 (2009).
[39] A.Yu.Okulov, Phys.Rev.A , **80**, 013837 (2009).
[40] L.Fallani,C.Fort,M.Inguscio.Adv.At.Mol.Opt.Phys.**56**, 119(2008).
[41] C.Nayak, S.H.Simon, A.Stern, M.Freedman, and S.D.Sarma, Rev.Mod.Phys. **80**,1083-1159 (2008) .
[42] Colloquium: Artificial gauge potentials for neutral

atoms". J.Dalibard, F.Gerbier, G.Juzeliunas, P.Ohberg,
Submitted to RMP,arXiv:1008.5378(2010) .